P. Gnaciński, M. Pepliński, A. Muc, D. Hallmann, P. Klimczak

Induction Motors under Voltage Fluctuations and Power Quality Standards

in
IEEE TRANSACTIONS ON ENERGY CONVERSION, vol. 39, no. 2, pp. 1255-1264, June 2024
DOI: 10.1109/TEC.2023.3342932

available at http:
https://ieeexplore.ieee.org/document/10360212
https://doi.org/10.1109/TEC.2023.3342932

Induction Motors under Voltage Fluctuations and Power Quality Standards

P. Gnaciński, *Member,* M. Pepliński, *Member, IEEE,* A. Muc, D. Hallmann, *Member, IEEE* and P. Klimczak

***Abstract*—Periodic voltage fluctuations are considered superposition of the fundamental harmonic and additional components, namely subharmonics and interharmonics (SaIs) —components of frequencies that are less than or not integer multiples of the fundamental frequency. Therefore, voltage fluctuations (VFs) occurring in real power systems are practical examples of various voltage SaIs. VFs and SaIs interconnected with them exert a harmful effect on rotating machinery, transformers, control systems, and electronic appliances. This study analyzes induction motors under VFs using experimental and finite element methods. The vibration and torque pulsations are compared for a single voltage subharmonic/interharmonic injection and VFs with various shapes of the modulating function. The results show that requirements concerning flicker severity, as well as the proposals to limit SaIs included in the standard IEEE-519:2022, do not protect induction motors against excessive vibration. Recommendations concerning the limitations of SaIs are formulated.**

***Index Terms* — AC motors, harmonic distortion, induction motors, standards, vibrations, voltage fluctuations.**

I. INTRODUCTION

VOLTAGE fluctuations are regarded as one of the most common and important power quality issues [1]-[3]. The fluctuations are usually caused by renewable energy sources [4]-[7] and double-frequency conversion systems such as inverters and high voltage DC links [8]-[12]. Another reason of their occurrence is current modulation originating from various fluctuating loads [4], [12], for example arc furnaces [4], welders [4], induction motors driving time-varying loads (e.g., piston compressors) [12], [13], [14], electronically controlled heaters [2], resistive automated spot welders [15], battery chargers for electrical vehicles [16], [17], and various office and household devices [4], [11], [18] – laser printers, dryers, copy machines, washing machines, etc.

Sinusoidal *VFs* can be considered as a superposition of the fundamental harmonic and two additional components [4], [15], [19] - [21]. One of them is of the interharmonic frequency (defined as the frequency that is not an integer multiple of the fundamental frequency [15]), and the other – of the subharmonic frequency (understood as the frequency less than the fundamental frequency [15]). Both the subharmonic and interharmonic components are of the same amplitude and their frequencies are symmetrical with respect to the fundamental frequency; for example, in a 50 Hz system, they could have frequencies of 30 and 70 Hz. Following [20], [22], such pairs are called symmetrical *SaIs* (*SSaIs*). Depending on the phase angle between voltage *SSaIs*, amplitude modulation (*AM*), phase modulation (*PhM*), and intermediate cases can be distinguished [4], [20], [22]. As *PhM* basically does not produce light flickers [20], *VFs* are usually assumed perfect *AM* [1], [18], [19], [21], [23] - [26]. However, any current modulation results in both *AM* and *PhM* [4].

Sinusoidal *VFs* are not frequently observed in a power system [1]. The most common fluctuations are rectangular, with step voltage changes [1], [26]. Notably, cyclic *VFs* of any shape can be analyzed as a superposition of sinusoidal fluctuations of various frequencies [19]. Accordingly, the fluctuations that are expected in real power systems [1], [15] can be regarded as practical examples of various voltage *SaIs*.

VFs exert a negative impact on various elements of power systems such as transformers, control systems, and electronic appliances [20], [27]. The impact is especially harmful in the case of rotating machinery [8], [10], [19], [21] - [24], [28] - [37]. In induction motors (*IMs*), *SaIs* cause local saturation of the magnetic circuit, an increase in power losses, speed fluctuations, overheating, excessive vibration, and torsional vibration, particularly under torsional resonance conditions. In *IMs* supplied with voltage containing *SaIs*, two kinds of torsional resonance may occur. The first is the rigid-body resonance [13], [19], in which the electromagnetic torque acts on the rotating mass as a torsional spring, and the torsional twist is insignificant [13]. The rigid-body resonance is reported to cause extraordinarily high vibration [22], [32], [36], torque pulsations [22], and an increase in windings temperature of approximately 20 K [34].

However, the elastic-body resonance is more harmful, leading to magnification of the torque pulsation, and consequently, drive train destruction [37], [38]. For example, in [37], fluctuations of the inverter output voltage (*SaIs*) caused pulsations with an amplitude of 0.75% in the motor torque. Because of resonance, the pulsations were amplified by a factor of 110 and induced coupling failures (twice within a few years) of the 7,000 hp induction motor. The most susceptible systems to torsional vibration are multi-megawatt drive trains with synchronous machines [8], [10]. Such drive trains are not found

(Corresponding author: Piotr Gnaciński).

P. Gnaciński, M. Pepliński and D. Hallmann are with the Department of Ship Electrical Power Engineering, Gdynia Maritime University, 81-87 Morska St., 81-225 Gdynia, Poland (e-mails: p.gnacinski@we.umg.edu.pl; m.peplinski@we.umg.edu.pl; d.hallmann@we.umg.edu.pl;).

A. Muc is with the Department of Ship Automation, Gdynia Maritime University, 81-87 Morska St., 81-225 Gdynia, Poland (e-mail: a.muc@we.umg.edu.pl).

P. Klimczak is with the Research and Development Centre for Electrical Machines, Zakład Maszyn Elektrycznych "EMIT" Cantoni Group, Narutowicza St. 72, Żychlin, Poland (e-mail: piotr.klimczak@cantonigroup.com).

in low-voltage systems, for which power quality standards should specify separate limits of voltage *SaIs*.

Since *VFs* were thought to particularly disturb light sources, their permissible levels [15], [39], [40] are determined based on the flicker severity indices, known as the short-term flicker severity P_{st} and the long-term flicker severity P_{lt} [15]. It should be stressed that both indices are based on the properties of incandescent bulbs, which are no longer being used in industry or household applications. At the same time, *LED* light sources are generally more resistant to *VFs* than incandescent bulbs [41], except certain frequencies of *VFs* [25], [41]. Additionally, for some *LEDs* no perceivable flickering is expected [41], [42]. For these reasons, the IEC/IEEE requirements on *VFs* may seem too restrictive. Moreover, they are incompatible with state-of-the-art technology.

It is also worth mentioning that the requirements concerning flickers are the only limitation set on *VFs* in power quality standards. The situation is worse in the case of single voltage *SaIs* because power quality standards generally do not specify their permissible levels. For instance, the *EN 50160* standard for *Voltage Characteristics of Electricity Supplied by Public Distribution Systems* [39] contains the following note regarding *SaIs*: "*Levels are under consideration, pending more experience*." In the *IEEE-519:2022 Standard for Harmonic Control in Electric Power Systems* [43], the reasons for *SaIs* limitation are considered in respect to the general shape of potential limit curves. Two alternative proposals of limit curves for non-generation installations are preliminarily formulated, using the IEC flickermeter and interharmonic subgroups definition [43]. The more restrictive curve establishes limits on *SaI* subgroups to 0.3%, and the others reach up to 0.5%. The main exceptions are *SaIs* of 50–70 Hz, with separate limits based on the flickermeter indications.

Modification of power quality standards and imposing limitations on *SaIs* requires in-depth investigations into their impact on various equipment, including *IMs*. Previous research on *IMs* under *SaIs* [19], [21] - [24], [28] - [37] has generally focused on currents, power losses, heating, torque pulsations, and speed fluctuations. The vibration under *SaIs* has only been examined in the authors' previous works (e.g., [22], [32], [36]), which were limited to *SaIs* of 1% (except [36]). Furthermore, the anterior studies generally concern either the effect of a single subharmonic/interharmonic component on *IMs* [21], [22], [28], [29], [31] - [36] or the effect of sinusoidal *VFs* (in practice, *SSaIs*) [19], [21] - [24]. The only exception is [30], which presented results on current, electromagnetic torque, and rotational speed under rectangular *VFs*. At the same time, some negative phenomena caused by *SaIs* (e.g., vibration and heating) are non-linear. Consequently, vibration under *VFs* that occur in real power systems cannot be fully predicted based on investigations of sinusoidal *AM* or a single voltage subharmonic/interharmonic.

In light of the above considerations, the objectives of this work have been determined. The paper aims to 1) assess whether *SaI* limits considered in *IEEE-519:2022 Standard for Harmonic Control in Electric Power Systems* [43] and requirements concerning flickers are sufficient to protect the induction motor from harmful vibration and 2) formulate recommendations for *SaI* limitations. Additionally, the vibration and torque pulsations are compared for a single voltage subharmonic/interharmonic injection and for *AM* using various shapes of the modulating function. The presented results include the case of *AM* corresponding to $P_{st} = 1$.

II. Voltage Fluctuation

VFs are usually understood as fast changes in the rms voltage value [1], [2], [4], and their chief cause is current variation [4]. The instantaneous voltage value $v(t)$ during current modulation can be described using the following equation (based on [4], [44]):

$$v(t) = V_{1A}[1 + m_v(t)]\cos[2\pi f_1 t + \varphi_v(t)] \quad (1)$$

where V_{1A} and f_1 are the amplitude and frequency of the fundamental voltage component, t is the time, and $m_v(t)$ and $\varphi_v(t)$ are functions modulating the amplitude and the phase of voltage, respectively [4]:

$$m_v(t) = -(RP_0 + XQ_0)m_c(t) + (XP_0 - RQ_0)\varphi_c(t) - LP_0\frac{dm_c(t)}{dt} - LQ_0\frac{d\varphi_c(t)}{dt} \quad (2)$$

$$\varphi_v(t) = (RQ_0 - XP_0)m_c(t) - (XQ_0 + RP_0)\varphi_c(t) - LQ_0\frac{dm_c(t)}{dt} + LP_0\frac{d\varphi_c(t)}{dt} \quad (3)$$

where R and X are per-unit fundamental-frequency source impedances at load terminals (Thevenin per-unit impedances), L is the per-unit source inductance, P_0 and Q_0 are per-unit non-fluctuating (average) active and reactive power, and $m_c(t)$ and $\varphi_c(t)$ the functions modulating the amplitude and the phase of the current, respectively, understood as in (4) [4]:

$$i(t) = I_{1A}[1 + m_c(t)]\cos[2\pi f_1 t - \psi + \varphi_c(t)] \quad (4)$$

where $i(t)$ is the instantaneous current value, I_{1A} is the amplitude of the fundamental current component, ψ is the phase angle.

The simplest case of *VFs* is sinusoidal. For sinusoidal *VFs*, the voltage waveform contains two frequency components in addition to the fundamental frequency (i.e., *SSaIs*) [4], [19], [20]:

$$v(t) = V_{1A}[\cos(2\pi f_1 t) + a\cos(2\pi f_{sh} t + \phi_{sh}) + a\cos(2\pi f_{ih} t + \phi_{ih})] \quad (5)$$

where a is the per-unit amplitude of voltage *SSaIs* (related to the fundamental voltage harmonic), ϕ_{sh} and ϕ_{ih} are phase angles of the subharmonic and interharmonic, f_{sh} and f_{ih} are the frequencies of the subharmonic and interharmonic components, respectively [4], [20]:

$$f_{ih} = f_1 + f_m \quad (6)$$

$$f_{sh} = f_1 - f_m \quad (7)$$

where f_m is the modulation frequency.

The above interharmonic component represents a positive sequence, whereas the sequence of the subharmonic component depends on f_m [12], resulting in a positive sequence for $f_m < f_1$ and negative for $f_m > f_1$ [12]. Furthermore, for $f_m > 2f_1$, this component appears as a negative-sequence interharmonic. It is

also worth mentioning that, if $\phi_{sh} + \phi_{ih} = 0$, the *VFs* take the form of *AM*, and if $\phi_{sh} + \phi_{ih} = 180°$, the *VFs* exhibit *PhM* [20].

In this study, special attention is paid to the rectangular modulation. In practice, this modulation may result from cyclic on-and-off switching of the load [1]. In a general case, its duty cycle [1], [40] may take on various percentages. Sample graphs of modulating functions for the duty cycle equal to 50% (symmetrical modulation) and 25% (asymmetrical modulation) are presented in Fig. 1. Corresponding voltage spectra are shown in Fig. 2 for f_m = 26 Hz and the relative voltage change (understood as a doubled amplitude of voltage modulation) [15], [40], δu = 0.94%. For this voltage change and the symmetrical modulation (Figs. 1a, 2a), the maximum value of a single subharmonic is u_{sh} = 0.3% (one of the possible limits considered in [43]). For the asymmetrical modulation (Figs. 1b, 2b), the maximum values of single *SaIs* are less than that for the symmetrical one, up to 0.21%. For these reasons, some tests presented in this study were performed for δu = 1.33%, corresponding to u_{sh} = 0.3% for the asymmetrical modulation. For the symmetrical modulation (Fig. 1a), the voltage spectrum (Fig. 2a) contains only *SaIs* resulting from the first harmonic of the modulating function (f_{sh} = 24 Hz, f_{ih} = 76 Hz) and odd harmonics (e.g., negative-sequence *SaIs* with f_{sh} = 28 Hz and f_{ih} = 80 Hz). Conversely, for the asymmetrical modulation (Fig. 1b), the spectrum (Fig. 2b) contains *SaIs* caused by even harmonics (e.g., negative-sequence *SaIs* with f_{sh} = 2 Hz and f_{ih} = 106 Hz).

A characteristic feature of another modulating function is the ramp changes in values [15]. A curve is presented in Fig. 3a (based on [15]) for the pulse width (defined as in [15]) equal to 10 ms, period T = 130 ms (f_m = 7.692 Hz), and the relative voltage change δu = 1.22%. The voltage spectrum corresponding to this modulating function is given in Fig. 3b. It contains six subharmonic components and numerous

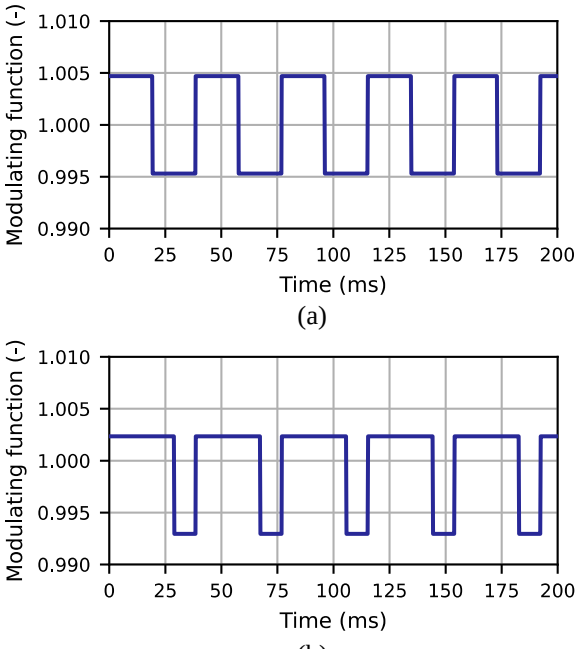

Fig. 1. Sample modulating functions for f_m = 26 Hz and a duty cycle equal to 50% (a) or 25% (b).

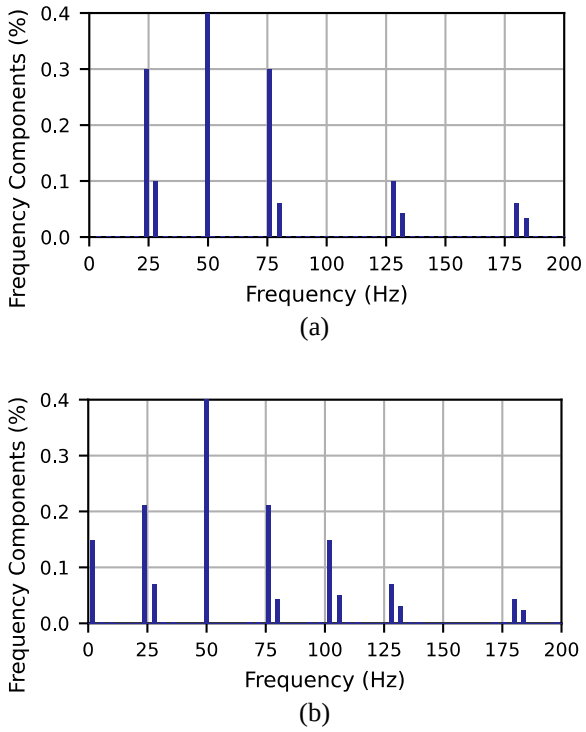

Fig. 2. Spectra of the voltage waveforms for the symmetrical modulating function presented in Fig. 1a (a) and asymmetrical modulating function shown in Fig. 1b (b).

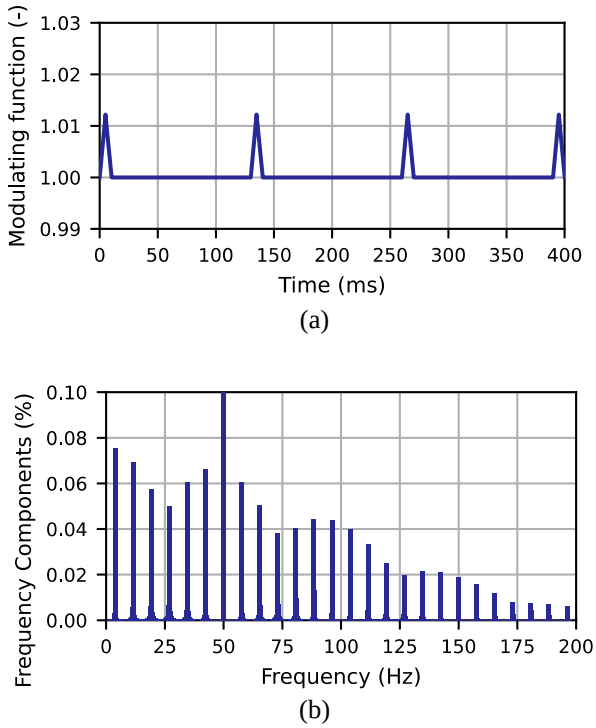

Fig. 3. Modulating function with ramp changes (a) and the corresponding voltage spectrum (b) for the modulation period T = 130 ms (f_m = 7.692 Hz).

TABLE I
NAMEPLATE PARAMETERS OF THE INVESTIGATED MOTORS

Motor	motor 1	motor 2	motor 3
Type	SLgm 315 ML2B	TSg100L-4B	1LE1003-1BB22-2AA4
Rated power (kW)	200	3	4
Rated frequency (Hz)	50	50	50
Rated voltage (V)	400	380	400
Rated current (A)	335	6.9	7.9
Rated power factor	0.90	0.81	0.82
Rated rotational speed (rpm)	2982	1415	1460

interharmonic ones with values of less than 0.1%.

The following sections discuss the investigations of *IMs* for the considered modulating functions.

III. METHODOLOGY

Investigations of *IMs* under *VFs* were performed using the finite element method (*FEM*) and experimental methods. For two-dimensional *FEM* analysis, the ANSYS Electronics Desktop environment (ANSYS Electromagnetics Suite 18.0.0) and the MAXWELL-ANSYS environment were used (ANSYS Electronics Desktop 2022R2). The numerical computations were performed for a 200 kW SLgm 315 ML2B motor (referred to as *motor 1*) and a 3 kW TSg100L-4B motor (referred to as *motor 2*) using a transient-type solver and tau-type meshes, consisting of 8,082 and 22,094 triangle elements, respectively. The parameters of the motor models were determined on the grounds of constructional data and empirical tests [33], [35]. One of the co-authors is on the staff of the manufacturer of *motor 1* (Zakład Maszyn Elektrycznych EMIT S.A. Cantoni Group) and participated in the design process of the motor. Details concerning the field models, including their validation for *motor 2* (*motor 1* was not tested experimentally because of its high rated power), are provided in [22], [32] - [34], and the nameplate parameters of the investigated motors are summarized in Table I.

The experimental setup consisted of a programmable power source, the *IMs* under investigation, a vibration measurement system, and a power quality analyzer. The AC power source, Chroma 61512+A615103, with a rated power of 36 kVA, enabled the generation of programmable power quality disturbances, including *AM* and injection of a single subharmonic/interharmonic component. Because of limitations of the power source, the research was restricted to *AM*. The measurement setup, aside from *motor 2*, contains a 4 kW cage induction motor, 1LE1003-1BB22-2AA4 (denoted as *motor 3*, see Table I), coupled with a *DC* generator. The vibration was measured using the Bruel & Kjaer (B&K) system, consisting of a standalone four-channel data acquisition module (B&K type: 3676-B-040), a three-axis magnetically-mounted accelerometer (B&K 4529-B of the following parameters: frequency range, 0.3–12,800 Hz; weight, 14.5 g; sensitivity, 10 mV/ms^2;

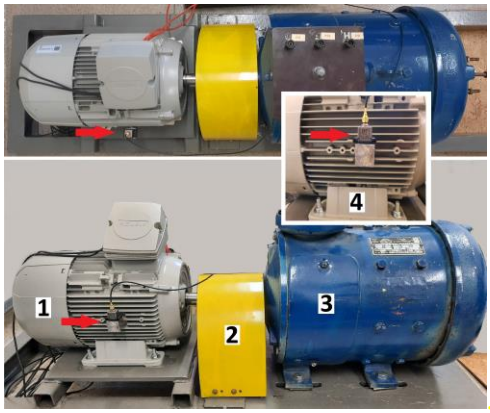

Fig. 4. Test bench of *motor 3*: 1 – induction motor, 2 – coupling cover, 3 – DC machine, 4 – accelerometer.

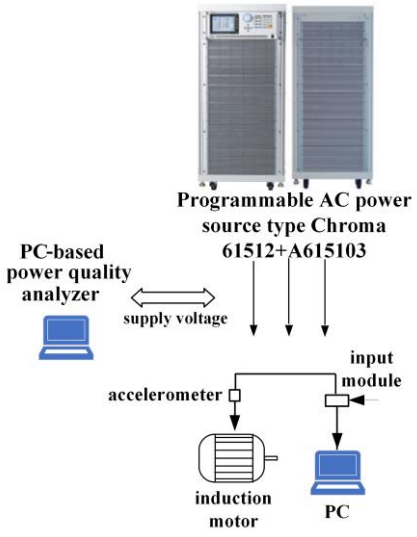

Fig. 5. Simplified diagram of the measurement stand.

maximum shock level peak, 5100 g), a calibrator (B&K 4294), and a computer with the B&K Connect software. Because the investigated motor is equipped with an aluminum casing, the accelerometer was mounted to additional steel stands and fixed to the motor (Fig. 4). A photograph of the laboratory setup is shown in Fig. 4, and a simplified diagram appears in Fig. 5 (based on [32]).

IV. ELECTROMAGNETIC TORQUE AND VIBRATION UNDER VOLTAGE FLUCTUATIONS

A. Assessment of Vibration Severity

To evaluate the vibration severity, the recommendations included in the standards were adopted [45], [46]. Depending on the broadband vibration velocity, four evaluation zones are distinguished [45], [46]: *Zone A* – the vibration falling within this zone generally occurs for newly commissioned machines, *Zone B* represents the vibration acceptable for unrestricted long-term operation, *Zone C* represents the vibration unacceptable for long-term continuous operation. The last evaluation zone is denoted as *Zone D*. According to the standard

[46], "*vibration values within this zone are normally considered to be of sufficient severity to cause damage to the machine*." As the boundaries of each evaluation zone are not univocally specified in the current standard [46], they were assumed using the previous version [45]. For machines of *Class I* (including electric motors with power not exceeding 15 kW), the upper boundary of *Zone A* is 0.71 mm/s. Furthermore, the vibration velocity between 0.71 and 1.8 mm/s falls into *Zone B*, and those between 1.8 and 4.5 mm/s fall into *Zone C*. Finally, the vibration velocity greater than 4.5 mm/s corresponds to *Zone D*.

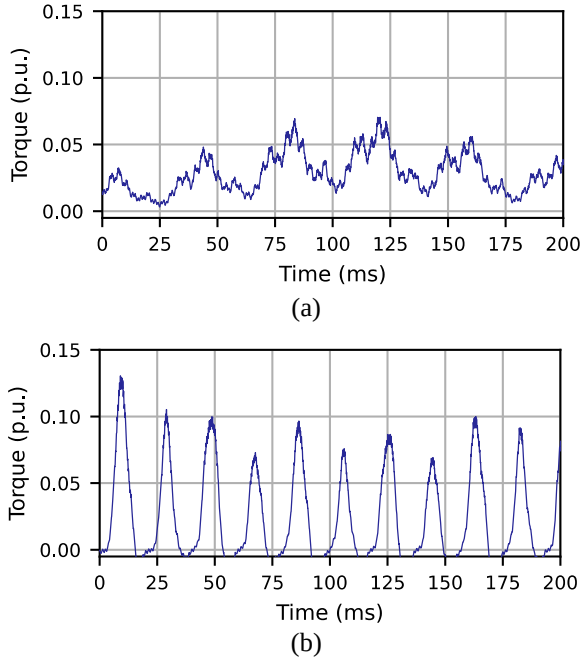

Fig. 6. Torque waveforms (related to the rated torque) for *motor 1* under *AM* for the voltage change δu = 0.94%, the modulation frequency f_m = 26 Hz, and the symmetrical (a) and asymmetrical (b) rectangular modulation.

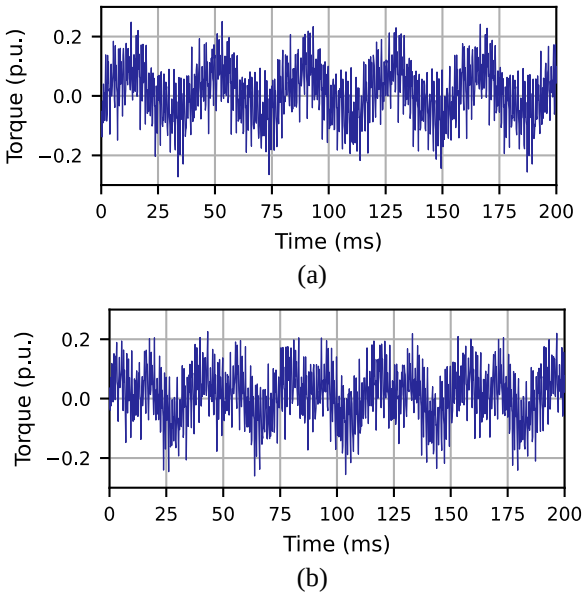

Fig. 7. Torque waveforms (related to the rated torque) for *motor 2* under *AM* for the voltage change δu = 94%, the modulation frequency f_m = 26 Hz, and the symmetrical (a) and asymmetrical (b) rectangular modulation.

B. Electromagnetic Torque

Pulsations of the electromagnetic torque are the main cause of excessive vibration in *IMs* under power quality disturbances (based on [36], [47]). For positive-sequence *SaIs*, the frequency of torque pulsations f_p is expressed as follows (based on [21]):

$$f_p = f_1 - f_{sh} \tag{8}$$

$$f_p = f_{ih} - f_1 \tag{9}$$

For the negative-sequence *SaIs*, the '−' sign occurring in (8) and (8) should be replaced with '+' [12].

The investigations in this subsection consider motors operating under no-load conditions, for which the highest vibration caused by *SaIs* was observed [22], [32], [36]. Notably, some motors experience no load for most of their operational life (e.g., under the standard duty type S6 15% [48]) or temporarily work under a very low load – for example prime movers of textile spinning mills, crushers and cable spooling systems [49], [50]. However, *IMs* usually work with much higher loads. Nevertheless, power quality requirements should protect all energy consumers from possible malfunctions caused by *SaIs*.

Figs. 6 and 7 show calculated torque waveforms for *motor 1* and *motor 2* under *AM*. The numerical computations were carried out for the negligible moment of inertia of the driven appliance [22], [32], [33], the frequency f_m = 26 Hz, the voltage

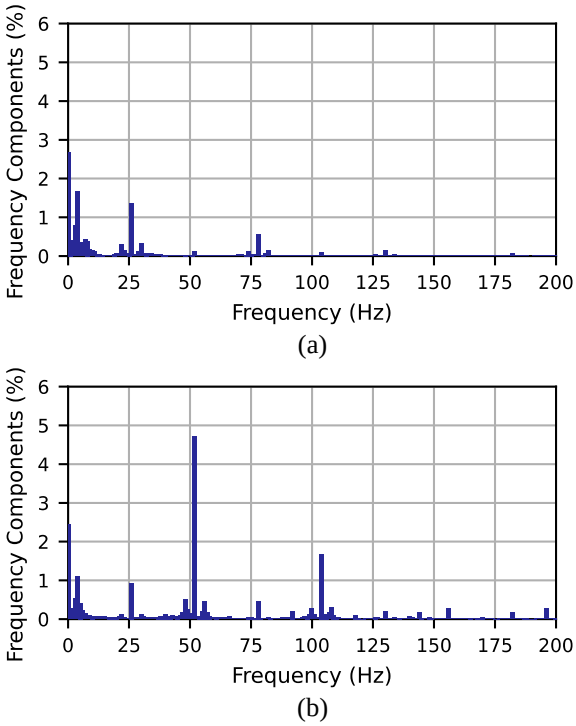

Fig. 8. Spectra of torque waveforms presented in Figs. 6a (a) and 6b (b) for *motor 1*. Frequency components are related to the rated torque.

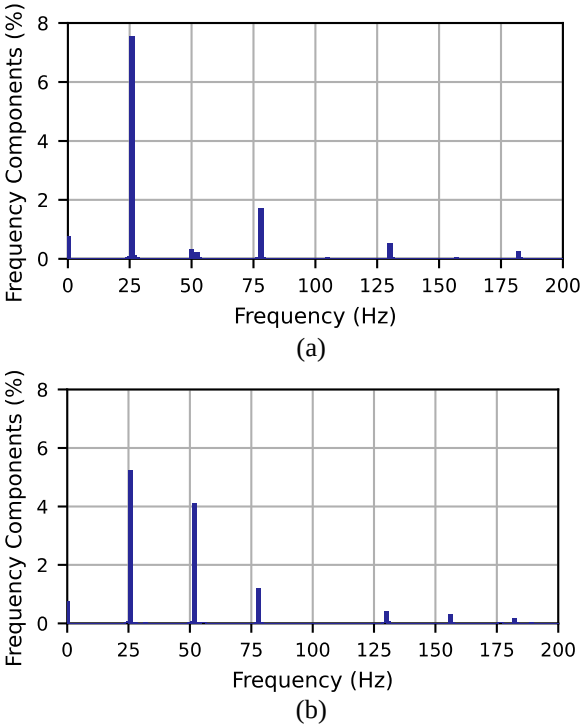

Fig. 9. Spectra of torque waveforms presented in Figs. 7a (a) and 7b (b) for *motor 2*. Frequency components are related to the rated torque.

change δu = 0.94%, and the rectangular modulation function of two duty cycles: 50% (symmetrical modulation, Fig. 1a) and 25% (asymmetrical modulation, Fig. 1b). The spectra of the torque waveforms are provided in Figs. 8 and 9 for *motor 1* and *motor 2*, respectively. For *motor 1* (Figs. 6 and 8) the torque component corresponding to the first harmonic of the modulating function (f_p = 26 Hz) is relatively small for both modulation cases. It is much smaller than the component caused by the second harmonic of the modulating function (f_p = 52 Hz, Fig. 8b), which results in a high amplitude of torque pulsations for the asymmetrical modulation (Fig. 6b). In contrast, for *motor 2* (Figs. 7 and 9), the highest torque component corresponds to the first harmonic of the modulating function. For the symmetrical modulation, the component is approximately 50% greater than that for the asymmetrical condition.

To sum up, any variation in the modulating function may significantly impact torque pulsations, and consequently, the vibration.

C. Vibration for Voltage Containing Single Subharmonic or Interharmonic

A complete picture of motor vibration under *SaIs* requires analysis for both single subharmonic/interharmonic components and voltage modulation. All results of experimental tests included in this subsection and the following subsections are presented for *motor 3*.

Fig. 10 shows the characteristic of the broadband vibration velocity versus the frequency of voltage subharmonics and

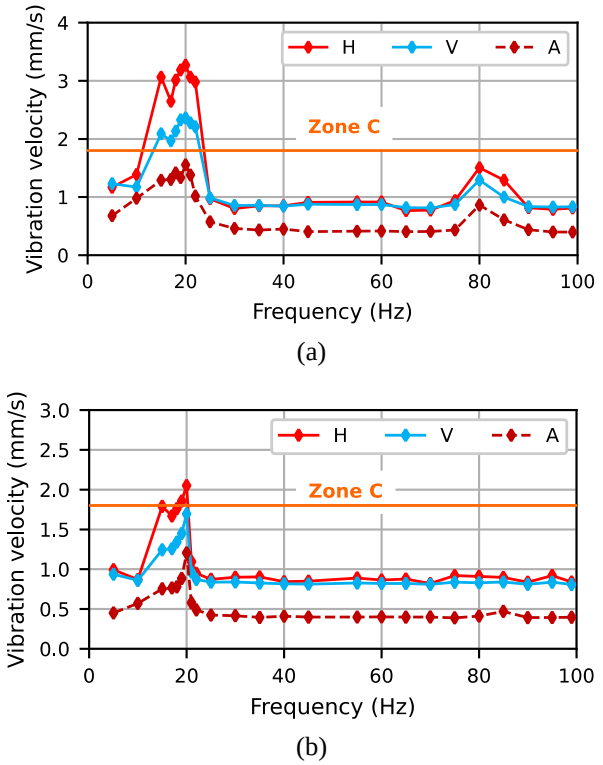

Fig. 10. Measured broadband vibration velocity in the horizontal (H), vertical (V), and axial (A) directions versus the frequency of voltage subharmonics and interharmonics $f_{sh/ih}$, for *SaIs* values of u_{sh}/i_{sh} = 0.3% (a) and u_{sh}/i_{sh} = 0.1% (b).

interharmonics, $f_{sh/ih}$, for no-load and two values of *SaIs*: $u_{sh/ih}$ = 0.3% and $u_{sh/ih}$ = 0.1%. The highest vibration occurs for the frequency f_{sh} of approximately 15–20 Hz, corresponding to rigid-body resonance [32], [36]. The vibration velocity reaches 3.269 mm/s for $u_{sh/ih}$ = 0.3%, and 2.051 mm/s for $u_{sh/ih}$ = 0.1%. For other frequencies, the vibration is generally below 1.5 mm/s. For comparison, the vibration velocity for the full load and $u_{sh/ih}$ = 0.3% is presented in Fig. 11. The vibration velocity is up to 1.051 mm/s and corresponds to *Zone B*.

Fig. 12 depicts the broadband vibration velocity under no-load, versus the subharmonic value for f_{sh} = 20 Hz. The vibration velocity exceeds the lower boundaries of *Zone C* (1.8 mm/s) for voltage subharmonics of $u_{sh} \approx$ 0.1%, which is three times less than the lower limit considered in the standard [43]. Furthermore, the vibration falls into *Zone D* (vibration velocity greater than 4.5 mm/s) for u_{sh} exceeding approximately 0.55%, and for u_{sh} = 0.7%, the vibration velocity reaches 6.851 mm/s. The measurements were not performed for subharmonics greater than 0.8% because of the risk of motor damage. The shape of the characteristic in Fig. 12 may be explained by coupling impact. We have observed similar characteristics for other motors coupled with *DC* generators, and the analogical characteristic was linear for an uncoupled 3 kW motor [36].

In summary, the vibration velocity may reach unacceptable levels for voltage *SaIs* within the limits considered in [43]. For the coupled motor, the vibration due to *SaIs* is non-linear.

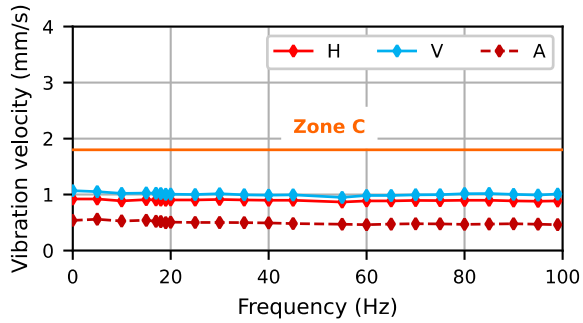

Fig. 11. Measured broadband vibration velocity in the horizontal (H), vertical (V), and axial (A) directions versus the frequency of voltage subharmonics and interharmonics $f_{sh/ih}$, for *SaIs* value of u_{sh}/i_{sh} = 0.3% and full load.

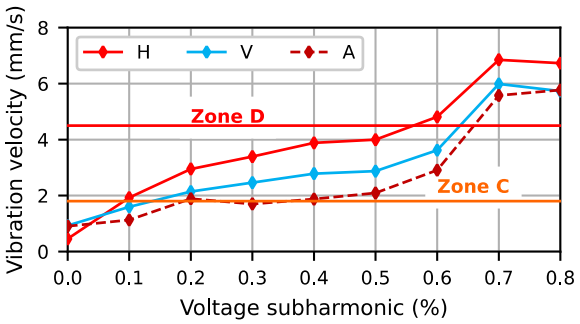

Fig. 12. Measured broadband vibration velocity in the horizontal (H), vertical (V), and axial (A) directions versus the value of the voltage subharmonic for the frequency f_{sh} = 20 Hz.

D. Vibration under Rectangular Voltage Modulation

This subsection presents the results of investigations on vibration under no-load and rectangular *AM* of the supply voltage, considered in Section II.

Fig. 13 shows the broadband vibration velocity for the symmetrical modulation (see Section II), and Figs. 14 and 15 depict it for the asymmetrical modulation. For the former, the assumed voltage change was δu = 0.94% (see Section II for justification), and for the latter, δu = 0.94% (Fig. 14) and δu = 1.33% (Fig. 15). For the symmetrical modulation, the vibration velocity reaches 2.7–2.8 mm/s for f_m = 30–40 Hz (Fig. 13). Furthermore, for the asymmetrical modulation and δu = 0.94%, the vibration velocity reaches 2.484 mm/s for f_m = 15 Hz (Fig. 14). The highest vibration occurs under asymmetrical *AM* and δu = 1.33% (Fig. 15). For f_m = 30 Hz and the horizontal direction, the maximum vibration velocity is 3.108 mm/s. Notably, the maximum vibration velocity exceeds the lower boundaries of *Zone C* for each of the considered cases.

The presented characteristics significantly differ in shape because of the non-linear vibration, various *SaIs* content for distinct modulating functions, and resonance phenomena. For example, for the symmetrical modulation and $f_{sh} \leq 25$ Hz, the vibration velocity is approximately 1.0 mm/s (Fig. 13). For the asymmetrical modulation and f_m = 15 Hz, the vibration velocity is 2.484 mm/s for δu = 0.94% (Fig. 14) and 2.603 mm/s for δu = 1.33% (Fig. 15). Of note, for the asymmetrical modulation and f_m = 15 Hz, the voltage waveform contains the subharmonic of f_{sh} = 20 Hz (caused by the second harmonic of the modulating function), which leads to rigid-body resonance.

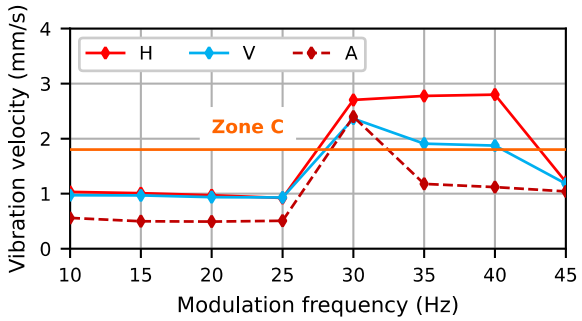

Fig. 13. Measured broadband vibration velocity for the voltage change δ_u = 0.94% in the horizontal (H), vertical (V), and axial (A) directions versus the frequency of the symmetrical rectangular voltage modulation.

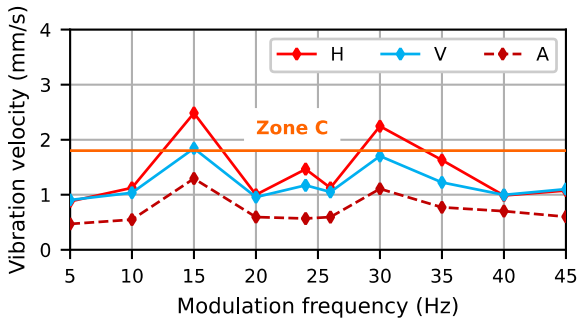

Fig. 14. Measured broadband vibration velocity for the voltage change δ_u = 0.94% in the horizontal (H), vertical (V), and axial (A) directions versus the frequency of the asymmetrical rectangular voltage modulation.

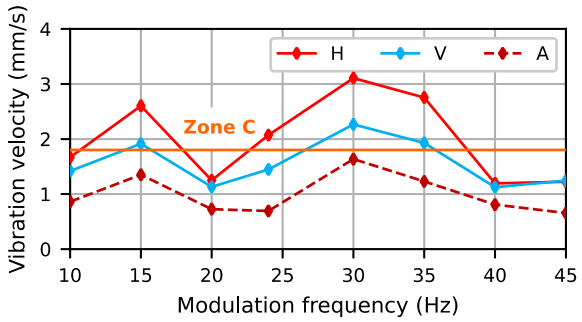

Fig. 15. Measured broadband vibration velocity for the voltage change δ_u = 1.33% in the horizontal (H), vertical (V), and axial (A) directions versus the frequency of the asymmetrical rectangular voltage modulation.

In summary, the *SaI* limits considered in [43] are far too tolerant. For the asymmetrical modulation, resonance phenomena can be expected for a wide range of f_m.

E. Vibration versus Short-Term Flicker Severity Pst

As mentioned in Section I, the only limitations of *VFs* are generally based on requirements concerning flicker severity.

In Figs. 16 and 17, the results of vibration measurements are provided for the modulation function with ramp changes (Fig. 3a) and no-load. It should be stressed that the empirical tests

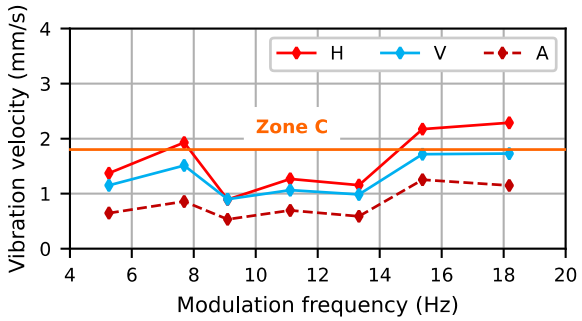

Fig. 16. Measured broadband vibration velocity in the horizontal (H), vertical (V), and axial (A) directions versus the modulation frequency, for the modulating function with ramp changes and $P_{st} = 1$.

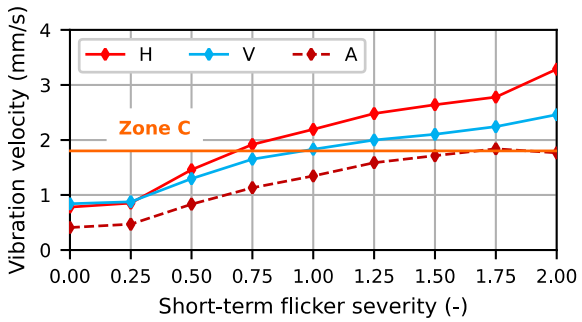

Fig. 17. Measured broadband vibration velocity in the horizontal (H), vertical (V), and axial (A) directions versus the short-term flicker severity P_{st}, for the modulating function with ramp changes and $f_m = 15.385$ Hz ($T = 65$ ms).

were carried out using the frequencies for which the human eye is relatively sensitive to flickers [4], [20].

Fig. 16 shows the vibration versus the frequency of f_m for the unitary short-term flicker severity P_{st}. For each measurement point, the appropriate δu was determined using the shape factor method [15]. The highest vibration velocity (up to 2.288 mm/s) is observed for $f_m > 15$ Hz. A local vibration peak also occurs for $f_m = 7.692$ Hz (the modulation period $T = 130$ ms) – the vibration velocity reaches 1.928 mm/s and falls into *Zone C*. Notably, this frequency is close to the frequency where the flicker curve is the most restrictive (8.8 Hz) [4], [15], [40]. The theoretical voltage spectrum for $f_m = 7.692$ Hz is given in Fig. 3b. As all voltage *SaIs* are below 0.1% (the lowest single subharmonic that may cause excessive vibration of the investigated motor, see Subsection C), the comparatively high vibration level probably results from a cumulative impact of *SaIs* with various frequencies. Fig. 17 presents the characteristic of the vibration velocity for $T = 65$ ms ($f_m = 15.385$ Hz) versus the short-term flicker severity P_{st}. The vibration velocity reaches the lower boundaries of *Zone C* for $P_{st} \approx 0.7$.

In summary, the results show that excessive vibration may occur for perfect *AM* of $P_{st} = 1$ and for the frequencies at which the human eye is especially sensitive to light flickers.

V. Discussion

Currently, the only established limitations of voltage *SaIs* are requirements concerning flicker severity [15], [39], [40]. It should be stressed that the limitations do not prevent excessive heating of *IMs*, transformer saturation, and mechanical resonance of turbo-generators caused by *SaIs* [20]. There are two reasons for this. First, *SSaIs* cause the most significant light flickers for perfect *AM*, whereas *PhM* flickers are practically unnoticeable [20]. At the same time, torque pulsations (being the main cause of excessive vibration under *SaIs*) can be much greater for *VFs* between *AM* and *PhM* than for perfect *AM* [22].

Second, the flickermeter is sensitive only to some frequencies of *VFs* [4], [20], which correspond with human eye-brain reaction [4], [20]. Section IV demonstrates that excessive vibration may also occur for perfect *AM* and for the frequencies at which the human eye is the most susceptible to flickers.

Although the requirements concerning flicker severity provide marginal protection for *IMs* against vibration, they should not be withdrawn or lowered without implementing strict requirements concerning *SaI* content.

Two alternative proposals of limit curves for non-generation installations are included in the *IEEE-519:2022 Standard for Harmonic Control in Electric Power Systems* [43]. The more restrictive curve generally limits *SaI* subgroups to 0.3%, and the other limits *SaIs* up to 0.5%. The results of Section III show that the considered limits are far too tolerant. To compound the problem, measurements of voltage *SaIs* are comparatively difficult [20], [43]. Because of spectral leakage, a single subharmonic/interharmonic tone can be split between neighboring *SaI* subgroups [20]. For example, the subharmonic of frequency 17.5 Hz occurs as two subgroups of the centered frequencies at 15 and 20 Hz, along with some minor components [20]. Consequently, when maintaining the limit of 0.3% for *SaI* subgroups, the real value of a single *SaI* tone may reach 0.45% (based on [20]). Similar situations can occur for the limit of 0.5%. Notably, for voltage subharmonics slightly exceeding this value, the vibration of the investigated motor falls into *Zone D* (u_{sh} of greater than approximately 0.55%). To sum up, implementation of the proposal included in [43] may result in vibration of unacceptable severity.

Far more strict proposals of *SaIs* limitation were included in [29], [31]. Ref. [29] proposed to limit any subharmonics to 0.1% to prevent excessive motor heating under the simultaneous presence of various power quality disturbances. In our experience [33], medium and high-power *IMs* are not exposed to overheating for subharmonics of less than 0.5% and frequencies greater than 10 Hz. Further, for *motor 2* (rated power of 3 kW), the sensitivity level with respect to heating is approximately 0.4% [34].

According to [31], voltage subharmonics should be limited to below 0.1% of the rated voltage. This proposal was justified by theoretical analysis of the motor torque-speed characteristics for the voltage subharmonic at 6 Hz. In our experience, voltage subharmonics of values reported in real power systems [7], [9] are not expected to disturb the start-up process of *IMs*. This issue may be the subject of future research.

In [28], it was noted that the magnetic circuit of *IMs* can become saturated by the voltage subharmonic. However, subsequent investigations (e.g., [24], [33], [36]) showed that an

increase in flux density is not the chief concern in *IMs* under subharmonics. The most important problems are vibration and torsional vibration [32], [33], [36], [37].

We believe that power quality standards should contain limits for both single *SaI* subgroups and an additional *SaI* index. As traces of *SaIs* can cause excessive vibration, this solution might help to mitigate measurement problems. This is inspired by the following comment concerning *SaI* limits in [43], "*IEC Flickermeter is necessary to assess voltage limits around the fundamental due to the difficulties in measuring very low voltage magnitudes.*" Similar to the flickermeter, an "*SaI meter*" can be developed and applied for any frequency. It should account for the cumulative impact of *SaIs* of various frequencies for selected harmful phenomena, for instance, the vibration of *IMs*.

To simplify measurements, the proposed device can only be sensitive to *AM*. Because real *VFs* are intermediate between *AM* and *PhM* (based on [4]), their indications should be multiplied by an appropriate correction factor. The value might depend on local grid properties (e.g., per-unit fundamental-frequency source impedances, see Section II).

The requirements concerning *SaIs* may follow regulations included in the standard [39], which specifies two permissible levels for some power quality disturbances, "*Under normal operating conditions the mean value of the fundamental frequency measured over 10 s shall be within a range of: …. for systems with no synchronous connection to an interconnected system (e.g. supply systems on certain islands): 50 Hz±2% (i.e. 49 Hz... 51 Hz) during 95% of a week; 50 Hz±15% (i.e. 42.5 Hz... 57.5 Hz) during 100% of the time.*" We believe that the lower limit of voltage *SaIs* (and indications of the proposed meter) should at least prevent *IMs* against vibration in *Zone C*, and the higher limit should prevent vibration in *Zone D*. The limit values, the most suitable aggregation intervals, the proposed meter and the percent of time corresponding to each limit may be subjects of future investigations. Additionally, the effect of motor power and number of poles on vibration can be studied.

VI. Conclusion

For more than 20 years, recommendations have been introduced for limits on voltage *SaIs* [29], [31]. However, the only current limitations on *SaIs* are requirements concerning flicker severity [15], [39], [40]. Although they provide marginal protection for *IMs* against vibration, the requirements should not be lowered or withdrawn without imposing strict limitations on *SaIs*.

The general shape of potential limit curves is discussed in [43]. Even for the lower limit (generally 0.3% for *SaI* subgroups), the vibration of *IMs* may reach unacceptable levels. To protect *IMs* against harmful vibration, some *SaIs* should be limited to less than 0.1%. In practice, measurement and precision errors may arise at such low limits.

One solution may be the development of an additional index, indicating the chosen phenomena caused by *SaIs*, for example, the vibration of *IMs*. In practice, the value of the index could be indicated by a dedicated device, similar to the flickermeter. To simplify measurements, the device could focus on *AM*, and its indications might be multiplied by an appropriate correction factor.

Power quality standards should contain two limit values (or limit curves) of voltage *SaIs* subgroups and two limit values for the proposed index, specified for different aggregation intervals. The higher limit should at least protect *IMs* against the vibration in *Zone D*, and the lower limit should protect against vibration in *Zone C*.

VII. References

[1] P. Kuwalek, "Estimation of parameters associated with individual sources of voltage fluctuations", *IEEE Transactions on Power Delivery*, vol. 36, no. 1, pp. 351-361, Feb. 2021.

[2] P. Kuwałek, "Selective identification and localization of voltage fluctuation sources in power grids", *Energies*, vol. 14, no. 20, pp. 6585, Oct. 2021.

[3] D. Patel and A. Chowdhury, "Mitigation of voltage fluctuation in distribution system using Sen transformer with variable loading conditions", in *2021 International Conference on Advances in Electrical, Computing, Communication and Sustainable Technologies (ICAECT)*, Bhilai, India, 2021, pp. 1-5.

[4] M. H .J. Bollen, and I. Y. H. Gu, "Signal processing of power quality disturbances", in *Wiley*: New York, USA, 2006, pp. 41–162.

[5] G. W. Chang et al. "A hybrid approach for time-varying harmonic and interharmonic detection using synchrosqueezing wavelet transform", *Applied Sciences*, vol. 11, no. 2, pp.752, 2021, 2021.

[6] V. Ravindran, T. Busatto, S. K. Rönnberg, J. Meyer and M. H. J. Bollen, „Time-varying interharmonics in different types of grid-tied PV inverter systems", *IEEE Transactions on Power Delivery*, vol. 35, no. 2, pp. 483-496, April 2020.

[7] X. Xie et al., "Characteristic analysis of subsynchronous resonance in practical wind farms connected to series-compensated transmissions", *IEEE Trans. Energy Convers*, vol. 32, pp.1117–1126, 2017.

[8] L. Bongini, and R. A. Mastromauro, "Subsynchronous torsional interactions and start-up issues in oil&gas plants: A real case study", in *AEIT International Annual Conference (AEIT)*, Firenze, Italy, 2019, pp. 1-6.

[9] A. B. Nassif, "Assessing the impact of harmonics and interharmonics of top and mudpump variable frequency drives in drilling rigs", *IEEE Transactions on Industry Applications*, vol. 55, no. 6, pp. 5574-5583, 2019.

[10] S. Schramm, C. Sihler, J. Song-Manguelle and P. Rotondo, "Damping torsional interharmonic effects of large drives*", IEEE Transactions on Power Electronics*, vol. 25, no. 4, pp. 1090-1098, April 2010.

[11] A. Testa et al., "Interharmonics: Theory and modeling", *IEEE Trans. Power Deliv.*, vol. 22, pp. 2335–2348, 2007.

[12] D. Zhang, W. Xu, and Y. Liu, "On the phase sequence characteristics of interharmonics", *IEEE Transactions on Power Delivery*, vol. 20, no. 4, pp. 2563-2569, 2005.

[13] A. Arkkio et al., "Additional losses of electrical machines under torsional vibration", *IEEE Trans. Energy Convers.*, vol.33, pp.245–251, 2018.

[14] B. A. Avdeev, et al., „Evaluation and procedure for estimation of interharmonics on the example of non-sinusoidal current of an induction motor with variable periodic load", *IEEE Access*, vol. 9, pp. 158412-158419, 2021.

[15] *IEEE Recommended Practice for the Analysis of Fluctuating Installations on Power Systems*, IEEE Std. 1453, 2015.

[16] S. M. Alshareef. "A novel smart charging method to mitigate voltage fluctuation at fast charging stations", *Energies*, vol. 15(5), 1746, 2022.

[17] P. Kuwałek, and G. Wiczyński, „Monitoring Single-Phase LV Charging of Electric Vehicles", *Sensors*, vol. 23.1, 141, 2023.

[18] E. Gutierrez-Ballesteros, S. Rönnberg, and A. Gil-de-Castro, „Characteristics of voltage fluctuations induced by household devices and the impact on LED lamps", *International Journal of Electrical Power & Energy Systems*, vol. 141: 108158, 2022.

[19] M. Ghaseminezhad et al., "High torque and excessive vibration on the induction motors under special voltage fluctuation conditions", *COMPEL - The International Journal for Computation and Mathematics in Electrical and Electronic Engineering*, vol. 40, no. 4, pp. 822-836, 2021.

[20] D. Gallo, C. Landi, R. Langella, and A. Testa, „Limits for low frequency interharmonic voltages: can they be based on the flickermeter use", in *IEEE Russia Power Tech*, St. Petersburg, Russia, pp. 1-7, June 2005.

[21] S. Tennakoon, S. Perera, and D. Robinson, “Flicker attenuation—Part I: Response of three-phase induction motors to regular voltage fluctuations”, *IEEE Trans. Power Deliv*., vol. 23, pp. 1207–1214, 2008.

[22] P. Gnaciński, D. Hallmann, A. Muc, P. Klimczak, and M. Pepliński, “Induction motor supplied with voltage containing symmetrical subharmonics and interharmonics”, *Energies*, vol. 15(20):7712, 2022.

[23] M. Ghaseminezhad et al., “Analysis of voltage fluctuation impact on induction motors by an innovative equivalent circuit considering the speed changes”, *IET Gener. Transm. Distrib.*, vol. 11, pp. 512–519, 2017.

[24] M. Ghaseminezhad et al., “An investigation of induction motor saturation under voltage fluctuation conditions”, *Journal of Magnetics*, vol. 22, pp. 306–314, 2017.

[25] M. Michalski, and G. Wiczyński, „Flicker dependency on voltage fluctuation at frequencies greater than power frequency”, in *20th International Conference on Harmonics & Quality of Power (ICHQP)*, Naples, Italy, 2022, pp. 1-5.

[26] P. Kuwałek, “IEC Flickermeter measurement results for distorted modulating signal while supplied with distorted voltage”, in *20th International Conference on Harmonics & Quality of Power (ICHQP)*, Naples, Italy, 2022, pp. 1-6.

[27] G. Crotti, G. D’Avanzo, P. S. Letizia and M. Luiso, “Measuring harmonics with inductive voltage transformers in presence of subharmonics”, *IEEE Transactions on Instrumentation and Measurement*, vol. 70, pp. 1-13, 2021.

[28] J. P. G. de Abreu, and A. E. Emanuel, “Induction motor thermal aging caused by voltage distortion and imbalance: loss of useful life and its estimated cost”, *IEEE Trans. on Industry Applications*, vol. 38 (1), pp. 12-20, 2002.

[29] J. P. G. De Abreu, and A. E. Emanuel, “The need to limit subharmonics injection”, in *Ninth International Conference on Harmonics and Quality of Power. Proceedings*, Orlando, FL, USA 2000, vol. 1, pp. 251-253.

[30] G. Bucci, E. Fiorucci, F. Ciancetta and N. Rotondale, „A testing system for the performance evaluation of electrical machines under realistic voltage fluctuations”, *IEEE Instrumentation & Measurement Technology Conference Proceedings*, Austin, Texas, USA, 2010, pp. 1441-1446.

[31] E. F. Fuchs, D. J. Roesler, M. and A. Masoum, “Are harmonic recommendations according to IEEE and IEC too restrictive?”, *IEEE Transactions on Power Delivery*, vol. 19(4), pp. 1775-1786, 2004.

[32] P. Gnaciński, D. Hallmann, P. Klimczak, A. Muc, and M. Pepliński, “Effects of voltage interharmonics on cage induction motors”, *Energies*, vol. 14 (5), pp. 1218, Feb. 2021.

[33] P. Gnaciński, and P. Klimczak, “High-power induction motors supplied with voltage containing subharmonics”, *Energies*, vol.13, pp. 5894, Nov. 2020.

[34] P. Gnaciński, M. Pepliński, D. Hallmann, and P. Jankowski, “The effects of voltage subharmonics on cage induction machine”, *International Journal on Electrical Power and Energy Systems*, vol. 111, pp. 125-131, 2019.

[35] P. Gnaciński, M. Pepliński, D. Hallmann, and P. Jankowski, “Induction cage machine thermal transients under lowered voltage quality”, *IET Electr. Power Appl.*, vol. 13, pp. 479–486, 2019.

[36] P. Gnaciński, M. Pepliński, L Murawski, and A. Szeleziński, “Vibration of induction machine supplied with voltage containing subharmonics and interharmonics”, *IEEE Trans. Energy Convers.*, vol. 34, pp. 1928–1937, 2019.

[37] H. Tripp, D. Kim, and R. Whitney, “A comprehensive cause analysis of a coupling failure induced by torsional oscillations in a variable speed motor”, in *Proc. of the 22nd Turbomachinery Symposium*, Texas A&M University, Turbomachinery Laboratories, USA, 1993, pp.17-24.

[38] R. X. Perez, “Design, modeling and reliability in rotating machinery”, in *Wiley*, Hoboken, NJ, USA, 2022.

[39] *Voltage characteristics of electricity supplied by public distribution network*, EN Standard 50160, 2010/A2:2019.

[40] *IEEE Recommended Practice—Adoption of IEC 61000-4-15:2010, Electromagnetic compatibility (EMC)—Testing and measurement techniques—Flickermeter—Functional and design specifications*, IEEE Std. 1453, 2011.

[41] A. Gil-de-Castro, S. K. Rönnberg, and M. H. Bollen, “Light intensity variation (flicker) and harmonic emission related to LED lamps”, *Electric Power Systems Research*, 146, 107-114, 2017.

[42] L. Sunny, and P. Philip, “Flicker free LED backlight driver with Passive Current Balancing and dimming function”, in *International Conference on Communication, Control and Information Sciences (ICCISc)*, Idukki, India, June 2021, vol. 1, pp. 1-6.

[43] *IEEE Standard for harmonic control in electric power systems*, IEEE Standard 519, 2022.

[44] *IEEE/IEC International Standard - Measuring relays and protection equipment - Part 118-1: Synchrophasor for power systems – Measurements*, - IEEE/IEC 60255-118-1, 2018.

[45] *Mechanical vibration -- Evaluation of machine vibration by measurements on non-rotating parts -- Part 1: General guidelines*, ISO Standard 10816-1, 1995.

[46] *Mechanical vibration — Measurement and evaluation of machine vibration — Part 1: General guidelines*, ISO Standard 20816-1, 2016.

[47] M. Tsypkin, “The origin of the electromagnetic vibration of induction motors operating in modern industry: Practical experience—Analysis and diagnostics”, *IEEE Transactions on Industry Applications*, vol. 53, no 2, pp.1669-1676, March-April 2017.

[48] *Rotating Electrical Machines. Part 1: Rating and Performance*, IEC Standard 60034-1, 2004.

[49] R. R. Singh, C. T. Raj, R. Palka, V. Indragandhi, M. Wardach, and P. Paplicki, „Energy optimal intelligent switching mechanism for induction motors with time varying load”, in *IOP Conference Series: Materials Science and Engineering*, Chennai, India, Aug. 2020, vol. 906, no. 1, p. 012017.

[50] R. R. Singh, and T. R. Chelliah, “Enforcement of cost-effective energy conservation on single-fed asynchronous machine using a novel switching strategy”, *Energy*, 126, 179-191, 2017.